



The congenital “ant-egg” cataract phenotype is caused by a missense mutation in connexin46

Lars Hansen,^{1,2} Wenliang Yao,³ Hans Eiberg,² Mikkel Funding,⁴ Ruth Riise,⁵ Klaus Wilbrandt Kjaer,^{1,2} James Fielding Hejtmancik,³ Thomas Rosenberg⁶

¹The Wilhelm Johannsen Centre for Functional Genome Research, Institute of Medical Biochemistry and Genetics and ²Institute of Medical Biochemistry and Genetics, Department G, Panum Institute, University of Copenhagen, Copenhagen, Denmark; ³Section on Ophthalmic Molecular Genetics, National Eye Institute, NIH, Bethesda, MD; ⁴Department of Ophthalmology, Aarhus University Hospital, Aarhus, Denmark; ⁵Department of Medical Genetics, Rikshospitalet University Hospital, Oslo, Norway; ⁶Gordon Norrie Centre for Genetic Eye Diseases, Kennedy Institute-National Eye Clinic, Hellerup, Denmark

Purpose: “Ant-egg” cataract is a rare, distinct variety of congenital/infantile cataract that was reported in a large Danish family in 1967. This cataract phenotype is characterized by ant-egg-like bodies embedded in the lens in a laminar configuration and is inherited as an autosomal dominant trait. We retrieved the family and performed linkage analysis to determine the disease locus and identify the mutated gene.

Methods: The family (CC00103) was identified in a National Register of Hereditary Eye Diseases and updated based on The Danish Civil Register System. Genome wide linkage analysis and haplotyping using STS marker systems were carried out to achieve a LOD score above 3. The disease-causing candidate gene was sequenced and the mutation was identified and verified by restriction enzyme digestion of genomic DNA from all individuals in family CC00103 and 60 healthy controls.

Results: Linkage analysis resulted in a LOD score of 3.91 for marker D13S1275 located close to the known cataract gene *GJA3*. A novel missense mutation c.32T>C (L11S), was found by sequencing DNA from two affected members. The mutation was present in all affected individuals and was neither found in unaffected family members nor in 60 healthy individuals by restriction enzyme digests.

Conclusions: The congenital “ant-egg” cataract phenotype is caused by a L11S mutation in connexin46 (Cx46) located in the signal peptide domain. Further studies are needed to unravel the mechanism leading to the formation of the “ant-eggs”.

Hereditary congenital and/or infantile cataracts (CC) exhibit extreme phenotypic variability as to lens opacities, giving rise to vivid designations such as stellate, pulverulent, floriform, pisciform, coralliform, or breadcrumb-like cataract. As regards localization within the lens substance, the most frequent morphological types of CC are confined to the nucleus, the lens sutures, the perinuclear layers (lamellar or zonular cataracts), the cortex, the anterior or posterior polar regions, or combinations of these [1].

Within families, the cataract phenotype often belongs to the same morphological category. “Ant-egg” cataract is an extremely rare phenotype, first described in a five generation family from Rostock, Germany [2,3]. A second family likewise exerting autosomal dominant transmission was reported from Graz, Austria in 1939 [4]. A third family of Danish extraction was presented by Riise in 1967 [5]. In addition an isolated case was published by Jaeger who introduced the name “Ameiseneierkatarakt” [6].

The “ant-egg” phenotype is a lamellar cataract with dense pearl-like or ant-egg-like structures imbedded in the lens, primarily confined to the perinuclear layers and to a lesser de-

gree in the fetal nucleus, leaving a clear cortical periphery. During and after lens extraction these extremely hard lens inclusions are liberated from the rest of the fragmented lens material and deposited in the anterior chamber, primarily on the anterior surface of the iris (Figure 1).

The mechanism leading to these peculiar formations have been subject to dispute. Riedl [4] held the opinion that the elements which he named “lentoids” were due to an abortive regeneration process originating from epithelial cells liberated during lens extraction. This hypothesis was supported by the observation of the formation of lentoids up to several years after lens extraction. However, unlike the other authors, Riedl did not have the opportunity to observe the cataracts prior to operation.

According to the opposed view, the ant-egg-like formations are the result of a degenerative process of the lens fibers surrounding the fetal nucleus [4,6]. In order to further elucidate the molecular mechanism behind the ant-egg formation we retrieved the Danish family in order to perform linkage and mutation analyses.

METHODS

Patients: The family (CC00103) was identified from a national register of hereditary eye diseases kept at the National Eye Clinic in Hellerup, Denmark. The pedigree (Figure 2A) was updated through The Danish Civil Registration System

Correspondence to: Thomas Rosenberg, PhD, Gordon Norrie Centre for Genetic Eye Diseases, Kennedy Institute-National Eye Clinic, 1 Rymarksvej, DK-2900 Hellerup, Denmark; Phone: +45 39452400; FAX: +45 39452420; email: roseeye@visaid.dk

kept by the Ministry of Interior Affairs and Health. After approval from the Scientific Ethical Committee the involved family members were addressed, and after informed written consent was obtained, venous blood was drawn from all affected members as well as their parents and siblings, if available. The updated family counted 43 members, 21 (10 affected and 11 unaffected) of whom were included in this investigation. The study adhered to the tenets of The Declaration of Helsinki.

DNA extraction: Blood samples were obtained from all available first-degree relatives. Genomic DNA was extracted from whole blood using standard procedures. Screening of the connexin46 gene (*GJA3*) for mutations and polymorphisms in the normal population was done on 60 independent persons selected from the Copenhagen Family Bank [7].

Linkage analysis: A complete genome-wide linkage scan was carried out using the ABI md-10 Linkage Mapping set and ABI3100 sequencer (Applied Biosystems, Foster City, CA)

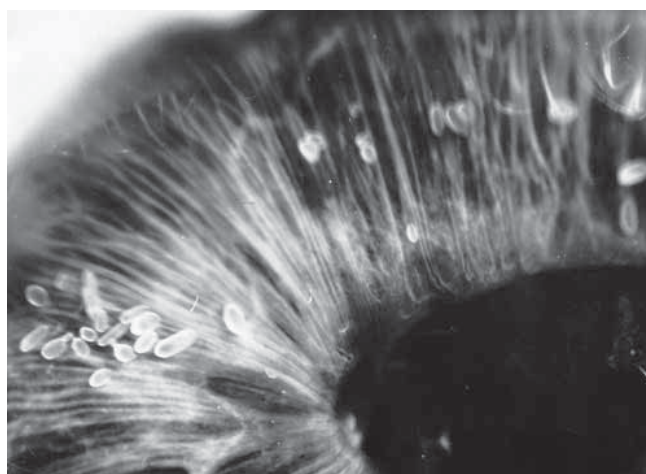


Figure 1. "Ant-Eggs" on the surface of the iris in an aphakic eye. The photography is from the original examination [5] in December 1965 of individual II:6 who carries the L11S mutation.

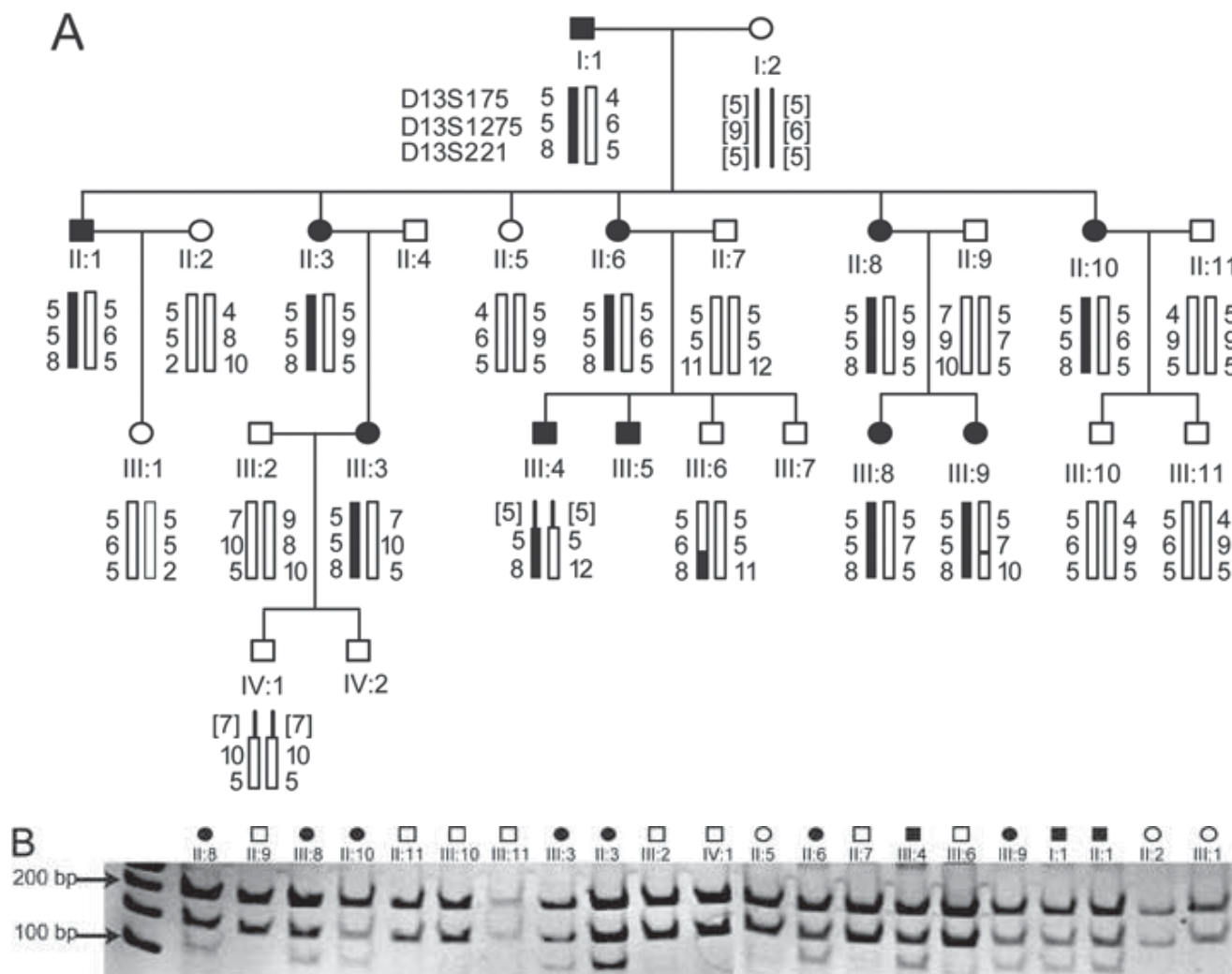


Figure 2. Pedigree of family CC00103 and restriction enzyme digests of the individuals. **A:** Only the affected branch of the family is shown. The disease haplotype is noted. Individuals II:2, II:6, and II:8 were analyzed by DNA sequencing, the remaining individuals were analyzed by restriction enzyme digestion analysis. **B:** Restriction enzyme (*Hpy188I*) digests of the 21 individuals from CC00103. Ten members carry the mutation and show three bands at 117 bp, 150 bp, and 200 bp, respectively. Unaffected individuals show two bands at 150 bp and 200 bp.

technology according to the manufacturer's protocol. Fine mapping was carried out for regions with LOD scores higher than 2 and additional STS markers were applied for the *GJA3* locus at chromosome 13. Standard conditions for γ -³³P-end-labeling of the forward PCR primers were used. (γ -³³P-ATP was purchased from Hartmann Analytic, Braunschweig, Germany) and T4-DNA-polynucleotide kinase from Fermentas (Vilnius, Lithuania). PCR standard conditions using the end-labeled PCR primer without further purification were carried out under the following conditions: 95 °C, 20 s, 55 °C, 20 s, and 72 °C for 30 s for 35 cycles using standard Taq-DNA polymerase (New England Biolabs, Ipswich, MA). Two point LOD scores for initial exclusion and mapping were calculated using the program LIPED [8].

DNA sequencing and diagnostic restriction enzyme digests: The genomic sequence of *GJA3* exon 2, and exon-intron border regions were bidirectional resequenced using BigDye version 1.1 sequencing technology (Applied Biosystems). The PCR primers (Table 1) were purchased from TAG Copenhagen A/S Copenhagen, Denmark and Taq DNA polymerases were purchased from various sources (HotStartTaq DNA Polymerase, Qiagen, Hilden, Germany; Taq DNA-polymerase, New England Biolabs; AmpliTaq Gold DNA Polymerase, Applied Biosystems; and Platinum Taq DNA polymerase, Invitrogen, Carlsbad, CA). Reactions were

carried out according to the manufacturer's protocols. The reaction volumes were a total of 15 μ l containing 2.5 μ M DNTP, 10 μ M of each primer, and 50-100 ng template DNA. Standard reaction conditions for all primer pairs were 95 °C for 5 min, 40 cycles 95 °C for 30 s, 56.4 °C for 30 s, and 72 °C for 1 min, followed by 5 min at 72 °C. PCR reactions were analyzed by 2% agarose gel-electrophoresis (1X TBE), by staining with ethidium bromide before sequencing. The mutation was analyzed by restriction enzyme digestion using *Hpy*188I (New England Biolabs) in a volume of 20 μ l using 2-4 μ l PCR product and 5-10 units of *Hpy*188I according to the manufacturer's protocol, and the products were analyzed by 20% acrylamide gel-electrophoresis (1X TBE). The PCR product was generated using primers Cx46_CC103_L11Sf and Cx46_ex2.2r (Table 1) under the same conditions as above. Sequence data were analyzed using standard software and alignments using ClustalW or BLAST and DNA sequences were aligned to GenBank NM_021954.

RESULTS

Genome wide linkage analysis of family CC00103 (Figure 2A) resulted in a LOD score of 3.91 for STS marker D13S1275 ($\theta=0.0$; Table 2). All affected individuals were carrying the disease haplotype and all unaffected individuals did not carry the haplotype. Close to D13S1275, 2.3 Mbp distal to the

TABLE 1.

Primer name	5' to 3' orientation	PCR product bp
CX46_ex2.1f	CCATCCCAGTACCATCCAG	
CX46_ex2.2r	CTCTTCAGCTGCTCCTCCTC	465
CX46_ex2.2f	CGAGAACGTCTGCTACGACA	
CX46_ex2.3r	CCTGCTTGAGCTTCTTCCA	515
CX46_ex2.3f	ACGGTGGACTGCTTCATCTC	
CX46_ex2.4r	CTCCCCTCCAGACTGCTG	590
CX46_ex2.4f	TCAAAGTCTAGCCCTGACC	
CX46_ex2.5r	ACCCCAAAGTCTCAGAAAGTG	643
CX46_ex2.5f	GGTTTCCGTGTTCAATGCTT	
CX46_ex2.1r	ATATCCTGGGCTTCACATGC	428
CX46_CC103_L11Sf	ATGGGCGACTGGAGCTTTCTGGG	

PCR and sequencing primers for the connexin46 gene (*GJA3*).

TABLE 2.

	Mbp	Distance to locus						
		0.0	0.01	0.05	0.10	0.20	0.30	0.40
<i>GJA3</i>	19.6	-	-	-	-	-	-	-
D13S175	19.7	1.49	1.47	1.36	1.22	0.92	0.57	0.21
D13S1275	21.8	3.91	3.85	3.58	3.23	2.46	1.59	0.65
D13S221	25.5	-∞	1.61	2.06	2.04	1.65	1.07	0.44

Two point LOD scores of family CC00103. Distances in Mega-bp (Mbp) are according to the UCSC, May, 2004, NCBI build 35.

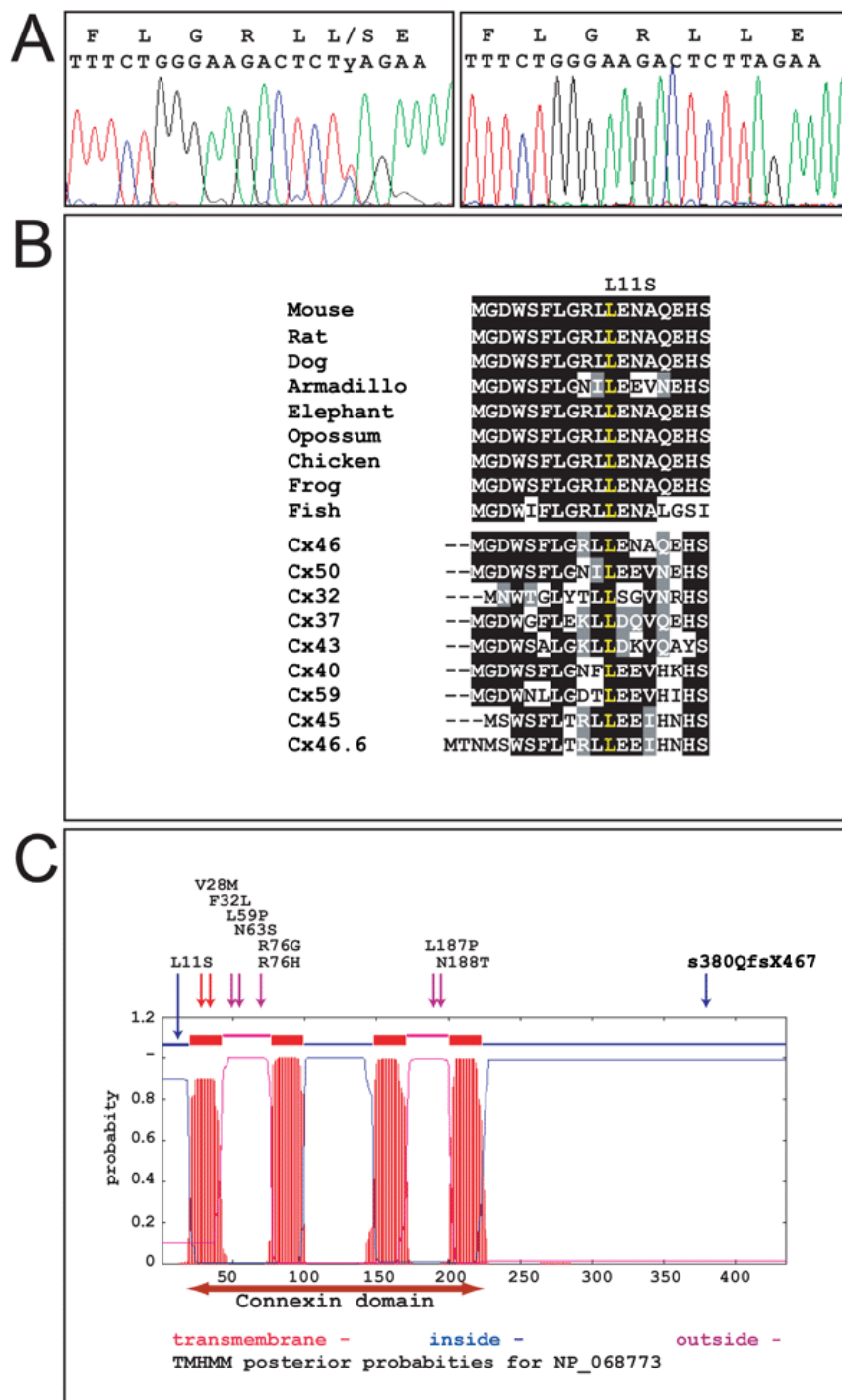


Figure 3. Protein sequence and structure of various connexins. **A**: Chromatogram of the *GJA3* DNA sequence from individual II:8 carrying the mutations (left) and an individual having wild type alleles. A double peak at position 32 represents the T>C transition and a shift of leucine to serine in the signal peptide.

B: ClustalW alignments of the first 18 amino acids of the signal peptide of Cx46 in various animals. The sequences are: mouse (*Mus musculus*), rat (*Rattus norvegicus*), dog (*Canis familiaris*), armadillo (*Armadillo officinalis*), elephant (*Loxodonta africana*), opossum (*Monodelphis domestica*), chicken (*Gallus gallus*), frog (*X_tropicalis*), and fish (*Tetraodon nigroviridis*). The DNA sequences used for translation are from the latest assemblies from GenBank and [23]. Below the aligned sequences for the different species are the aligned signal peptide sequences for 9 different human connexin proteins. Cx46 and Cx50 are the only lens-specific expressed proteins. The conserved leucine at position 11 is marked in yellow. The human sequences are derived from the following GenBank accession numbers: Cx46, NP_068773; Cx50, NP_005258; Cx32, NP_000157; Cx37, NP_002051; Cx43, NP_000156; Cx40, NP_005257; Cx59, NP_110399; Cx45, NP_005488; and Cx46.6, NP_065168 [23].

C: Prediction of the transmembrane helices in the Cx46 protein shown in graphics. The location and orientation of domains in the primary protein structure are shown on the X-axis and the probability for forming helices is shown on the Y-axis [10]. Cytoplasmatic, transmembrane, or extracellular regions are shown in color on top of the plot. A horizontal red two-headed arrow below the plot indicates the conserved connexin-domain. All known human Cx46 mutations [13-19] are denoted above the plot. Transmembrane mutations are identified by red arrows, mutations in the cytoplasmatic regions are identified by blue arrows, and mutations in the extracellular domains are identified by violet arrows.

TABLE 3.

Nucleotide	Amino acid codon	Protein or mRNA position	Individuals		dbSNP
			II:2	II:8	
c.895C>A	L299M	IC3	AA	AA	rs968566
c.1017G>A	A339A	IC3	GA	GG	rs1161741
c.1551G>A	-	3'UTR	GA	GA	rs4769953
c.1627G>T	-	3'UTR	GA	GG	rs1886176

(*GJA3*) exon2 polymorphisms in family CC00103. In the "Protein or mRNA position" column, IC3 indicates intracellular domain 3 and 3'UTR indicates a 3' untranslated region.

marker, the gap junction protein alpha 3 gene (*CX46*, *GJA3*) is located. Sequencing of the coding exon 2 revealed the mutation c.32T>C, (L11S; Figure 3A). Restriction enzyme analysis by digest with *Hpy*188I demonstrated that all affected persons in family CC00103 carried the mutation and all unaffected did not (Figure 2B). Further restriction digestion among 60 unrelated controls did not detect the mutation. The mutation at position 32 in the coding region changes the codon TTA for leucine to the codon TCA for serine. Prediction of cleavage sites and a signal peptide using SignalP 3.0 based on a combination of several artificial neural networks and hidden Markov models [9] suggest a most likely cleavage site between position 41 and 42. The mutation L11S is in this signal peptide, which is responsible for trafficking of the gap junction protein through the endoplasmic reticulum (ER) and the Golgi apparatus to the cell membrane. The structure of the Cx46 protein as predicted by TMHMM Server (version 2.0) [10] is in accordance with a four-transmembrane model conserved among all gap junction proteins (Figure 3C). ClustalW alignment of the translated NH₂-signal peptide in Cx46 demonstrate that the L11 position is conserved among 10 different organisms and further that the L11 position is conserved in 8 of the human connexin genes (Figure 3B). Four known polymorphisms were found in the two sequenced individuals II:2 and II:8 (Table 3).

DISCUSSION

Four reports, three of which are light microscopic, deal with the histological morphology of lens ant-eggs obtained during operations. Stock [3] examined an extracted lens as well as solitary pearl-like structures. These structures of which the largest measured 0.34 mm were loosely embedded in the lens nucleus without any connection with the surrounding degenerated lens fibers. They had a slightly rugged mulberry-like surface and consisted of a laminar structure with deposits of calcium carbonate. In a later histological study [4] the size of the "lentoids" was estimated between 40 μm and 240 μm, the majority, however, measured between 130-160 μm. A capsule surrounded most "lentoids". They had a layered composition of parallel thread-like fibers reaching from one end of the lentoid to the other. Each fiber had a flattened prismatic form and measured 4x8 μm in cross-section. A few small and degenerate nuclei were present in some of the fibers. The authors considered the formation of "lentoids" as a failed attempt at regeneration [4]. Nissen and Schroeder [11] extended the Danish family with another generation and added three new cases. They also undertook a histologic examination of the globular ant-egg-like structures and observed a central calcified core surrounded by a lightly stained homogeneous material. At the border between the core and the surrounding area a transition zone with densely toluidine-staining material

TABLE 4.

Nucleotide	Amino acid codon	Protein Domain	Phenotype	Reference
c.1A>G	M1I	Start codon	Not known	rs9578255
c.32T>C	L11S	SP	Ant-Egg cataract	This study
c. 82G>A	V28M	TM1	Variable expression	[11]
c.956C>A	F32L	TM1	Nuclear pulverulent	[16]
c.176C>T	P59L	EC1	Nuclear punctuate	[13]
c.188A>G	N63S	EC1	Zonular pulverulent	[14]
c. 227G>A	R76H	EC1	Pulverulent	[12]
c.226C>G	R76G	EC1	Total	[11]
c.560C>T	P187L	EC2	Zonular pulverulent	[17]
c.563A>C	N188T	EC2	Nuclear pulverulent	[15]
c.1137insC	S380QfsX467	IC3	Zonular pulverulent	[14]

Known mutations in *GJA3* exon2. In the "Protein domain" column, SP indicates a signal peptide, TM refers to a transmembrane domain, EC indicates an extracellular domain, and IC refers to an intracellular domain.

was seen. An energy dispersive analysis revealed a high content of phosphorus together with calcium throughout the “ant-egg”. Finally, the latter authors performed an electron microscopic examination [12]. They observed membrane-limited cytoplasmic bodies in the transition zone as well as the surrounding area. These inclusion bodies were often continuous with linear five-layered structures that most likely represented a fusion of two adjacent membranes and were interpreted as derived from either the smooth endoplasmic reticulum or represented more or less collapsed lysosomes involved in autophagocytosis or secretion vacuoles.

The L11S transversion is the first mutation found in the signal peptide of Cx46; all other known mutations (Table 4) are located in either the conserved four-transmembrane connexin domain, the two cysteine-containing extracellular domains, or in the cytoplasmic COOH-terminus (Figure 3C) [13-19]. All mutations are missense mutations except for S380QfsX476 (S380QfsX476 is caused by the mutation c.1137insC, a frame shift mutation in codon 379 and codon S380 is the first affected amino acid) [16] (Figure 3C).

Aberrant location to the ER and/or Golgi has been shown for the Cx46 frame shift mutation S380QfsX467 [20]. Minogue et al. [20] verified experimentally that the wild type Cx46 protein and the truncated Cx46S380X protein were directed to the plasma membrane and assembled into functional gap junctions, while the Cx46S380QfsX467 fusion protein was allocated to ER or Golgi compartments in transfected HeLa cells. Very elegantly they demonstrated that a diphenylalanine-motif within the last 29 amino acids of the COOH-terminus of the S380QX467 extension of Cx46 was responsible for the aberrant trafficking of the mutated protein as observed in several chimeric constructs.

Interestingly, most hitherto known Cx46 cataract phenotypes are described as punctuate or pulverulent. These tiny spots might represent small calcified tissue elements.

The L11 position in Cx46 is conserved among many organisms and in human connexin genes (Figure 3B). A corresponding G12S mutation in the signal peptide of the Cx32 protein (Figure 3B) [21] shows similarities with the phenotype observed for the ant-egg cataract. Martin et al. [21] proved that the mutated Cx32-G12S protein was not properly directed to the cell membrane, but was mainly present at intracellular stores located adjacent to the nuclei. Double immunostaining using antibodies to Cx32 and to p58, a cellular marker of the Golgi compartment, demonstrated a predominantly Golgi location for the Cx32-G12S mutation. It is tempting to draw an analogy to the Cx46-L11S mutation found in combination with the ant-egg cataract resulting in a dislocation of the protein and accumulation within a cytoplasmic compartment. This supposition is supported by electron microscopic observations [12]. The high calcium and phosphorus content in the “ant-eggs” and the nature of the crystals [12] is in agreement with the presence of calmodulin-binding domains in the NH₂-terminal first 21 amino acids of Cx32 [22]. It is therefore likely that a corresponding calmodulin-binding domain, which is a Ca²⁺-binding protein that mediates many Ca²⁺-dependent pro-

cesses, also is present in Cx46 and is involved in the high calcium-content of the “ant-eggs”.

The detailed mechanism involved in the formation the large calcified accumulations of degenerate lens fibers, which constitutes the ant-egg-like structures remains obscure.

ACKNOWLEDGEMENTS

We thank the family for their participation. Jeanette Andreasen and Annemette Mikkelsen performed excellent technical assistance. The Wilhelm Johannsen Centre for Functional Genomics and the Genome Group/RC-LINK hosted the project and the Danish National Research Foundation funds the Wilhelm Johannsen Centre for Functional Genomics. The project was supported by grants from The Danish Association of the Blind and The Danish Eye Health Society. RC-Link is supported by The Danish Medical Research Council.

REFERENCES

- Amaya L, Taylor D, Russell-Eggitt I, Nischal KK, Lengyel D. The morphology and natural history of childhood cataracts. *Surv Ophthalmol* 2003; 48:125-44.
- Axenfeld, K. Bericht ber die achtundzwanzigste Versammlung der Ophthalmologischen Gesellschaft, Heidelberg 1900. Hess, W. and Leber, T. 1901. Wiesbaden, Verlag von J.F.Bergmann.
- Stock W. Beitrage zur angeborenen Starbildung. *Klin Monatsbl Augenheilkd* 1902; 40:11-8.
- Riedl F. Eigenartige Form von Linsenregeneration (multiple freie Lentoidbildung) bei Cataracta secundaria in einer Familie mit Cataracta pernuclearis hereditaria. *Klin Monatsbl Augenheilkd* 1939; 103:169-93.
- Riise R. Hereditary “ant-egg-cataract”. *Acta Ophthalmol (Copenh)* 1967; 45:341-6.
- Jaeger W. “Ameiseneierkatarakt”. *Ber Dtsch Ophthal Ges* 1964; 66:368-73.
- Eiberg H, Nielsen LS, Klausen J, Dahlen M, Kristensen M, Bisgaard ML, Moller N, Mohr J. Linkage between serum cholinesterase 2 (CHE2) and gamma-crystallin gene cluster (CRYG): assignment to chromosome 2. *Clin Genet* 1989; 35:313-21.
- Ott J. A computer program for linkage analysis of general human pedigrees. *Am J Hum Genet* 1976; 28:528-9.
- Bendtsen JD, Nielsen H, von Heijne G, Brunak S. Improved prediction of signal peptides: SignalP 3.0. *J Mol Biol* 2004; 340:783-95.
- Krogh A, Larsson B, von Heijne G, Sonnhammer EL. Predicting transmembrane protein topology with a hidden Markov model: application to complete genomes. *J Mol Biol* 2001; 305:567-80.
- Nissen SH, Schroder HD. Ant-egg cataract. A study of a family with dominantly inherited congenital (ant-egg) cataract, including a histological examination of the formed elements. *Acta Ophthalmol (Copenh)* 1979; 57:14-9.
- Schroder HD, Nissen SH. Ant-egg cataract. An electron microscopic study. *Acta Ophthalmol (Copenh)* 1979; 57:435-42.
- Devi RR, Reena C, Vijayalakshmi P. Novel mutations in GJA3 associated with autosomal dominant congenital cataract in the Indian population. *Mol Vis* 2005; 11:846-52.
- Burdon KP, Wirth MG, Mackey DA, Russell-Eggitt IM, Craig JE, Elder JE, Dickinson JL, Sale MM. A novel mutation in the Connexin 46 gene causes autosomal dominant congenital cataract with incomplete penetrance. *J Med Genet* 2004; 41:e106.

Erratum in: J Med Genet 2005; 42:288.

15. Bennett TM, Mackay DS, Knopf HL, Shiels A. A novel missense mutation in the gene for gap-junction protein alpha3 (GJA3) associated with autosomal dominant "nuclear punctate" cataracts linked to chromosome 13q. *Mol Vis* 2004; 10:376-82.
16. Mackay D, Ionides A, Kibar Z, Rouleau G, Berry V, Moore A, Shiels A, Bhattacharya S. Connexin46 mutations in autosomal dominant congenital cataract. *Am J Hum Genet* 1999; 64:1357-64.
17. Li Y, Wang J, Dong B, Man H. A novel connexin46 (GJA3) mutation in autosomal dominant congenital nuclear pulverulent cataract. *Mol Vis* 2004; 10:668-71.
18. Jiang H, Jin Y, Bu L, Zhang W, Liu J, Cui B, Kong X, Hu L. A novel mutation in GJA3 (connexin46) for autosomal dominant congenital nuclear pulverulent cataract. *Mol Vis* 2003; 9:579-83.
19. Rees MI, Watts P, Fenton I, Clarke A, Snell RG, Owen MJ, Gray J. Further evidence of autosomal dominant congenital zonular pulverulent cataracts linked to 13q11 (CZP3) and a novel mutation in connexin 46 (GJA3). *Hum Genet* 2000; 106:206-9.
20. Minogue PJ, Liu X, Ebihara L, Beyer EC, Berthoud VM. An aberrant sequence in a connexin46 mutant underlies congenital cataracts. *J Biol Chem* 2005; 280:40788-95.
21. Martin PE, Mambetisaeva ET, Archer DA, George CH, Evans WH. Analysis of gap junction assembly using mutated connexins detected in Charcot-Marie-Tooth X-linked disease. *J Neurochem* 2000; 74:711-20.
22. Torok K, Stauffer K, Evans WH. Connexin 32 of gap junctions contains two cytoplasmic calmodulin-binding domains. *Biochem J* 1997; 326:479-83.
23. Kent WJ, Sugnet CW, Furey TS, Roskin KM, Pringle TH, Zahler AM, Haussler D. The human genome browser at UCSC. *Genome Res* 2002; 12:996-1006.